Performance of four high-order shock-capturing schemes for stiff source terms with discontinuities: preliminary results

By D. V. Kotov, H. C. Yee, B. Sjögreen, W. Wang AND C.-W. Shu

1. Motivation and objectives

The overarching goal of this work is to develop efficient and highly accurate high-order numerical methods for magnetized turbulence with strong shocks and finite-rate chemistry/combustion. Numerical simulation is challenging because of the conflicting requirements for numerical methods to be accurate enough to resolve the small scales of (magnetized) turbulence but robust enough to handle shock waves without generating spurious numerical noise. Furthermore, the different physics models have different time scales, that, when underresolved, might interact numerically to produce erroneous results. In modeling non-equilibrium flow problems containing finite-rate chemistry or combustion, the appearance of the source terms poses additional numerical difficulties beyond that for solving non-reacting turbulent flows. The added numerical method challenges are stiffness and nonlinearity of source terms. However, here only stiff source terms are addressed. For stiff reactions it is well known that the wrong propagation speed of discontinuities occurs due to the under-resolved numerical solutions in both space and time (LeVeque & Yee 1990).

In addition to the minimization of numerical dissipation while maintaining numerical stability in compressible turbulence with strong shocks, (Yee & Sweby 1997; Yee *et al.* 1999*b*; Yee & Sjögreen 2002; Yee 2002; Yee & Sjögreen 2007; Yee *et al.* 2008) discussed a general framework for the design of such schemes. Yee & Sjögreen (2010), Sjögreen & Yee (2009*b*) and Wang *et al.* (2012) and references cited therein present their recent progress on the subject. In (Yee *et al.* 2011), a short overview of this recent progress is given.

The objective of the present technical report is to a gain a deeper understanding of the behavior and performance of four high-order shock-capturing schemes for two representative stiff detonation wave problems. The test cases consist of the Arrhenius 1D Chapman-Jouguet (C-J) detonation wave and a 2D Heaviside detonation wave. These are the same two test cases considered in Wang *et al.* (2012). The considered four schemes are the fifth-order WENO, "WENO5", the Wang *et al.* (2012) newly developed subcell resolution version of WENO5, "WENO5/SR", the Yee et al. nonlinear filter version of WENO5, "WENO5fi" and the Durcros split version of WENO5fi, "WENO5fi+split" (Yee & Sjögreen 2007; Yee *et al.* 2008; Yee & Sjögreen 2010; Sjögreen & Yee 2009*a*). For the temporal discretization, the classical fourth-order Runge-Kutta method (RK4) is used. See the aforementioned references for the development of these schemes.

WENO5/SR (Wang *et al.* 2012) is a modified fractional step method that solves the convection step and reaction step separately. In the convection step, any high-order shock-capturing method can be used. In the reaction step, an ODE solver is applied but with the computed flow variables in the shock region modified by the Harten subcell resolution idea (Harten 1989).

WENO5fi is the filter version of WENO5. On the first stage a full time step by RK4 is performed. For this stage the sixth-order central spatial base scheme is used. On the second stage the solution is filtered by the dissipative portion of WENO5 in conjunction with a wavelet flow sensor. The wavelet flow sensor indicates the locations where shock-capturing dissipations are needed and leaves the remaining region free of numerical dissipation contamination. WENO5fi+split is WENO5fi applied to the Ducros *et al.* (2000) split form of the governing equation before the application of WENO5fi. The Ducros et al. split form is a preprocessing step to condition the governing equation(s) before the application of high-order central schemes for improved numerical stability. This process is widely used in numerical modeling and simulation of turbulent flows.

The comparison of the performance of the four schemes is largely based on the degree that each method captures the correct location and jump size of the reaction front for coarse grids. It is remarked that, in order to resolve the sharp reaction zone, many grid points in this zone are still needed. The behavior of these schemes in the vicinity of a sharp reaction zone with several levels of grid refinement briefly are touched upon below.

2. 2D reactive Euler equations

Consider the 2D reactive Euler equations with two chemical states of burnt gas and unburnt gas and a single irreversible reaction. Without heat conduction and viscosity, the system can be written as

$$\rho_t + (\rho u)_x + (\rho v)_y = 0, \tag{2.1}$$

$$(\rho u)_t + (\rho u^2 + p)_x + (\rho uv)_y = 0, \tag{2.2}$$

$$(\rho v)_t + (\rho uv)_x + (\rho v^2 + p)_y = 0, \tag{2.3}$$

$$E_t + (u(E+p))_x + (v(E+p))_y = 0, \tag{2.4}$$

$$(\rho z)_t + (\rho uz)_x + (\rho vz)_y = -K(T)\rho z, \tag{2.5}$$

where $\rho(x, y, t)$ is the mixture density, $u(x, y, t)$ and $v(x, y, t)$ are the mixture x- and y-velocities, $E(x, y, t)$ is the mixture total energy per unit volume, $p(x, y, t)$ is the pressure, $z(x, y, t)$ is the mass fraction of the unburnt gas, $K(T)$ is the chemical reaction rate, and $T(x, y, t)$ is the temperature. The pressure is given by

$$p = (\gamma - 1)(E - \frac{1}{2}\rho(u^2 + v^2) - q_0\rho z), \tag{2.6}$$

where the temperature $T = \frac{p}{\rho}$ and q_0 is the chemical heat released in the reaction.

The reaction rate $K(T)$ is modeled by an Arrhenius law

$$K(T) = K_0 \exp\left(\frac{-T_{ign}}{T}\right), \tag{2.7}$$

where K_0 is the reaction rate constant and T_{ign} is the ignition temperature. The reaction rate may be also modeled in the Heaviside form

$$K(T) = \begin{cases} 1/\varepsilon & T \geq T_{ign} \\ 0 & T < T_{ign} \end{cases}, \tag{2.8}$$

where ε is the reaction time and $1/\varepsilon$ is roughly equal to K_0.

3. Numerical methods

The newly developed high-order finite difference method with subcell resolution (WENO5/SR) for advection equations with stiff source terms (Wang *et al.* 2012) in 2D is briefly summarized in section (3.1). Then the key aspects of the filter counterpart of the WENO schemes are discussed in section (3.2).

3.1. *High-order finite difference methods with subcell resolution for advection equations with stiff source terms*

The general fractional step approach based on Strang-splitting (Strang 1968) for equation

$$U_t + F(U)_x + G(U)_y = S(U) \tag{3.1}$$

is as follows. The numerical solution at time level t_{n+1} is approximated by

$$U^{n+1} = A\left(\frac{\Delta t}{2}\right) R(\Delta t) A\left(\frac{\Delta t}{2}\right) U^n. \tag{3.2}$$

The reaction operator R is over a time step Δt and the convection operator A is over $\Delta t/2$. The two half-step reaction operations over adjacent time steps can be combined to save cost. In order to obtain more accurate results in the reaction zone we can also use one reaction step via N_r sub steps, i.e.,

$$U^{n+1} = A\left(\frac{\Delta t}{2}\right) R\left(\frac{\Delta t}{N_r}\right) \cdots R\left(\frac{\Delta t}{N_r}\right) A\left(\frac{\Delta t}{2}\right) U^n \tag{3.3}$$

in some numerical examples studied in (Wang *et al.* 2012).

The convection operator A is defined to approximate the solution of the homogeneous part of the problem on the time interval, i.e.,

$$U_t + F(U)_x + G(U)_y = 0, \quad t_n \le t \le t_{n+1}. \tag{3.4}$$

The reaction operator R is defined to approximate the solution on a time step of the reaction problem:

$$\frac{dU}{dt} = S(U), \quad t_n \le t \le t_{n+1}. \tag{3.5}$$

Here, the convection operator consists of, e.g., WENO5 with Roe flux and RK4 for time discretization. If there is no smearing of discontinuities in the convection step, any ODE solver can be used as the reaction operator. However, all the standard shock-capturing schemes will produce a few transition points in the shock when solving the convection equation. These transition points are usually responsible for causing incorrect numerical results in the stiff case. Thus we cannot directly apply a standard ODE solver at these transition points. Here the Harten's subcell resolution technique in the reaction step is employed. The general idea is as follows. If a point is considered a transition point of the shock, information from its neighboring points which are deemed not transition points, will be used instead. In 2D case, we apply the subcell resolution procedure dimension by dimension. The algorithm proceeds as follows.

(1) Use a shock indicator to identify cells in which discontinuities are believed to be situated. One can use any indicator suitable for the particular problem. We consider the minmod-based shock indicator in (Harten 1989; Shu & Osher 1989). Identify a troubled cell I_{ij} in both the x- and y-directions by applying the shock indicator to the mass fraction z. Define the cell I_{ij} as troubled in the x-direction if $|s^x_{ij}| \ge |s^x_{i-1,j}|$ and $|s^x_{ij}| \ge |s^x_{i+1,j}|$

with at least one strict inequality, where

$$s_{ij}^x = \text{minmod}\{z_{i+1,j} - z_{ij}, z_{ij} - z_{i-1,j}\}. \tag{3.6}$$

Similarly we can define the cell I_{ij} as troubled in the y-direction if $|s_{ij}^y| \geq |s_{i,j-1}^y|$ and $|s_{ij}^y| \geq |s_{i,j+1}^y|$ with at least one strict inequality where

$$s_{ij}^y = \text{minmod}\{z_{i,j+1} - z_{ij}, z_{ij} - z_{i,j-1}\}. \tag{3.7}$$

If I_{ij} is troubled only in one direction, we apply the subcell resolution along this direction. If I_{ij} is troubled in both directions, we choose the direction that has a larger jump. Namely, if $|s_{ij}^x| \geq |s_{ij}^y|$, subcell resolution is applied along the x-direction, otherwise it is done along the y-direction. In the following steps (2)-(3), without loss of generality, we assume the subcell resolution is applied in the x-direction. Assuming I_{ij} is troubled in the x-direction, we apply subcell resolution along the x-direction.

In a troubled cell identified above, we continue to identify its neighboring cells. For example, we can define $I_{i+1,j}$ as troubled if $|s_{i+1,j}^x| \geq |s_{i-1,j}^x|$ and $|s_{i+1,j}^x| \geq |s_{i+2,j}^x|$ and similarly define $I_{i-1,j}$ as troubled if $|s_{i-1,j}^x| \geq |s_{i-2,j}^x|$ and $|s_{i-1,j}^x| \geq |s_{i+1,j}^x|$. If the cell $I_{i-q,j}$ and the cell $I_{i+r,j}$ $(q, r > 0)$ are the first good cells from the left and the right (i.e., $I_{i-q+1,j}$ and $I_{i+r-1,j}$ are still troubled cells), we compute the fifth order ENO interpolation polynomial $p_{i-q,j}(x)$ and $p_{i+r,j}(x)$ for the cells $I_{i-q,j}$ and $I_{i+r,j}$, respectively.

(2) Modify the point values z_{ij}, T_{ij}, and ρ_{ij} in the troubled cell. To define the modified values we use reconstruction by the ENO interpolation polynomials

$$\begin{cases} \tilde{z}_{ij} = p_{i-q,j}(x_i; z), & \tilde{T}_{ij} = p_{i-q,j}(x_i; T), & \tilde{\rho}_{ij} = p_{i-q,j}(x_i; \rho), & \text{if } \theta \geq x_i \\ \tilde{z}_{ij} = p_{i+r,j}(x_i; z), & \tilde{T}_{ij} = p_{i+r,j}(x_i; T), & \tilde{\rho}_{ij} = p_{i+r,j}(x_i; \rho), & \text{if } \theta < x_i \end{cases}, \tag{3.8}$$

where the location θ is determined by the conservation of energy E

$$\int_{x_{i-1/2}}^{\theta} p_{i-q,j}(x; E)dx + \int_{\theta}^{x_{i+1/2}} p_{i+r,j}(x; E)dx = E_{ij}\Delta x. \tag{3.9}$$

Under certain conditions, it can be shown that there is a unique θ satisfying Eq. (3.9), which can be solved using, for example, a Newton's method. If there is no solution for θ or there is more than one solution, we choose $\tilde{z}_{ij} = z_{i+r,j}$, $\tilde{T}_{ij} = T_{i+r,j}$ and $\tilde{\rho}_{ij} = \rho_{i+r,j}$. For particular problems one can choose any other suitable method for the reconstruction.

(3) Use modified values $\tilde{z}_{ij}$, $\tilde{T}_{ij}$ and $\tilde{\rho}_{ij}$ instead of U_{ij} in the ODE solver if the cell I_{ij} is a troubled cell. For simplicity, explicit Euler is used as the ODE solver.

$$(\rho z)_{ij}^{n+1} = (\rho z)_{ij}^n + \Delta t S(\tilde{T}_{ij}, \tilde{\rho}_{ij}, \tilde{z}_{ij}). \tag{3.10}$$

3.2. *Well-balanced high order filter schemes for reacting flows*

Before the application of a high-order non-dissipative spatial base scheme, the preprocessing step to improve stability had split inviscid flux derivatives of the governing equation(s) in the following three ways, depending on the flow types and the desire for rigorous mathematical analysis or physical argument.

- Entropy splitting (Olsson & Oliger 1994) and (Yee *et al.* 2000; Yee & Sjögreen 2002). The resulting form is non-conservative and the derivation is based on entropy norm stability with numerical boundary closure for the initial value boundary problem.
- The system form of the Ducros *et al.* (2000) splitting. This is a conservative splitting and the derivation is based on physical arguments.
- Tadmor entropy conservation formulation for systems (Sjögreen & Yee 2009*a*). The

derivation is based on mathematical analysis. It is a generalization of Tadmor's entropy formulation to systems and has not been fully tested on complex flows.

When strong shocks are present one should use the conservative splitting. Therefore, for all the WENO5fi+split computations shown here, the Ducros et al. splitting is employed.

After the application of a non-dissipative high-order spatial base scheme on the split form of the governing equation(s), to further improve nonlinear stability of the non-dissipative spatial base scheme, the post-processing step of (Yee & Sjögreen 2007, 2010; Sjögreen & Yee 2004) nonlinearly filtered the solution by a dissipative portion of a high-order shock-capturing scheme with a local wavelet flow sensor. The flow sensor provides locations and amounts of built-in shock-capturing dissipation that can be further reduced or eliminated. The idea of these nonlinear filter schemes for turbulence with shocks is that, instead of relying solely on very high-order high-resolution shock-capturing methods for accuracy, these nonlinear filter schemes (Yee *et al.* 1999*a*, 2000; Sjögreen & Yee 2004; Yee & Sjögreen 2007) take advantage of the effectiveness of the nonlinear dissipation contained in good shock-capturing schemes as stabilizing mechanisms (a post-processing step) at locations where needed. The nonlinear dissipative portion of a high-resolution shock-capturing scheme can be any appropriate shock-capturing scheme. By design, the flow sensors, spatial base schemes and nonlinear dissipation models are standalone modules. See (Yee & Sjögreen 2010, 2011) for the recent improvements of the work (Yee *et al.* 1999*a*, 2000; Sjögreen & Yee 2004; Yee & Sjögreen 2007) that are suitable for a wide range of flow speeds with minimal tuning of scheme parameters. The subcell resolution approach using the fractional step procedure can carry over to the aforementioned filter schemes. Some attributes of the high-order filter approach are:

- Spatial base scheme: High-order and conservative (no flux limiter or Riemann solver)
- Physical viscosity: Contribution of physical viscosity, if it exists, is automatically taken into consideration by the base scheme in order to minimize the amount of numerical dissipation to be used by the filter step
- Efficiency: Unlike standard shock-capturing and/or hybrid shock-capturing methods, the nonlinear filter method requires one Riemann solve per dimension per time step, independent of time discretizations. The nonlinear filter method is more efficient than its shock-capturing method counterparts, employing the same order of the respective methods.
- Accuracy: Containment of numerical dissipation via a local wavelet flow sensor
- Well-balanced scheme: These nonlinear filter schemes are well-balanced schemes for certain chemical reacting flows, i.e. they are able to exactly preserve specific steady-state solutions of the governing equations (Wang *et al.* 2011)
- Parallel algorithm: suitable for most current supercomputer architectures

4. Numerical examples

The behavior of the considered four methods (i.e. WENO5, WENO5/SR, WENO5fi, WENO5fi+split) is investigated on two test cases that were considered in (Wang *et al.* 2012). The test cases consist of the Arrhenius 1D C-J detonation wave and a 2D Heaviside detonation wave. Note that the numerical results presented here could be slightly different from (Wang *et al.* 2012) because of the minor differences in the numerical schemes, e.g. different choice of variables.

4.1. *Chapman-Jouguet (C-J) detonation wave (Arrhenius case)*

The first test case is the C-J detonation wave (Arrhenius case) (Helzel *et al.* 1999; Tosatto & Vigevano 2008). The initial values consist of totally burnt gas on the left-hand side and totally unburnt gas on the right-hand side. The density, velocity, and pressure of the unburnt gas are given by $\rho_u = 1$, $u_u = 0$, and $p_u = 1$. The initial state of the burnt gas is calculated from C-J condition, see e.g. (Chorin 1976):

$$p_b = -b + (b^2 - c)^{1/2}, \tag{4.1}$$

$$\rho_b = \frac{\rho_u[p_b(\gamma+1) - p_u]}{\gamma p_b}, \tag{4.2}$$

$$S_{CJ} = [\rho_u u_u + (\gamma p_b \rho_b)^{1/2}]/\rho_u, \tag{4.3}$$

$$u_b = S_{CJ} - (\gamma p_b/{}_r h o_b)^{1/2}, \tag{4.4}$$

where

$$b = -p_u - \rho_u q_0(\gamma - 1), \tag{4.5}$$

$$c = p_u^2 + 2(\gamma - 1)p_u\rho_u q_0/(\gamma + 1). \tag{4.6}$$

The heat release $q_0 = 25$ and the ratio of specific heats is set to $\gamma = 1.4$. The ignition temperature $T_{ign} = 25$ and $K_0 = 16418$. The computational domain is $[0, 30]$. Initially, the discontinuity is located at $x = 10$. At time $t = 1.8$, the detonation wave has moved to $x = 22.8$. The reference solution is computed by the regular WENO5 scheme with 10000 uniform grid points and CFL=0.05. Figure 1 shows the pressure and mass fraction comparison among the standard WENO5 scheme, WENO5/SR, WENO5fi and WENO5fi+split using 50 uniform grid points. For this particular problem and grid size, WENO5fi+split compares well with WENO5/SR for the computed pressure solution. Calculation by the WENO5/SR and WENO5fi+split can capture the correct structure using fewer grid points than those in (Helzel *et al.* 1999; Tosatto & Vigevano 2008). A careful examination of the mass fraction solutions indicates that WENO5fi+split is one grid point ahead of the discontinuity location when compared with the reference solution. The reference solution is obtained by WENO5 using $10,000$ grid points. Because WENO5fi+split is less dissipative than WENO5, the restriction of the shock-capturing dissipation using the wavelet flow sensor helps to improve the wrong propagation speed of discontinuities without the subcell resolution procedure. Figure 2 shows a grid refinement in the hope of resolving the narrow reaction zone using 800 uniform grid points. It is interesting to see that the WENO5fi+split scheme produces oscillatory solutions in the vicinity of the reaction front. This behavior prompted us to perform a systematic uniform grid refinement study using six levels ($200, 400, 800, 1600, 3200$ and 6400 points). As the number of grid point increases, this oscillatory behavior in the vicinity of the reaction front becomes more pronounced. However, for the more dissipative scheme WENO5, as we refine the grid, the computed solution becomes increasingly close to the reference solution. For WENO5/SR, the oscillatory solution near the reaction zone as the grid is refined is small compared with that in the WENO5fi+split scheme.

4.2. *2D detonation waves*

The second example is taken from (Bao & Jin 2000). The chemical reaction is modeled by the Heaviside form with the parameters

$$\gamma = 1.4, \quad q_0 = 0.5196 \times 10^{10}, \quad \frac{1}{\varepsilon} = 0.5825 \times 10^{10}, \quad T_{ign} = 0.1155 \times 10^{10}$$

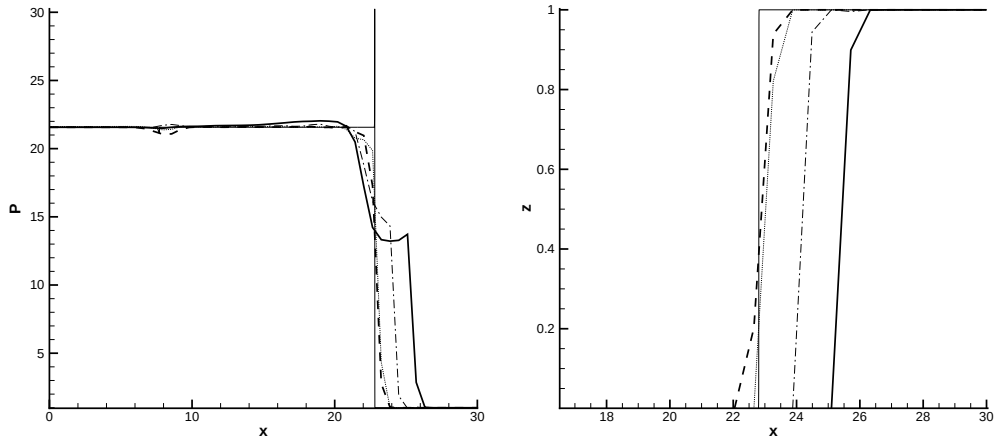

FIGURE 1. Pressure and mass fraction comparison among four high-order shock-capturing methods for the C-J detonation problem, Arrhenius case at $t = 1.8$ using 50 uniform grid points, CFL=0.1 and $N_r = 2$. Thin solid line: reference solution; thick solid line: WENO5; dashed line: WENO5/SR; dashed-dot line: WENO5fi; dot line - WENO5fi+split.

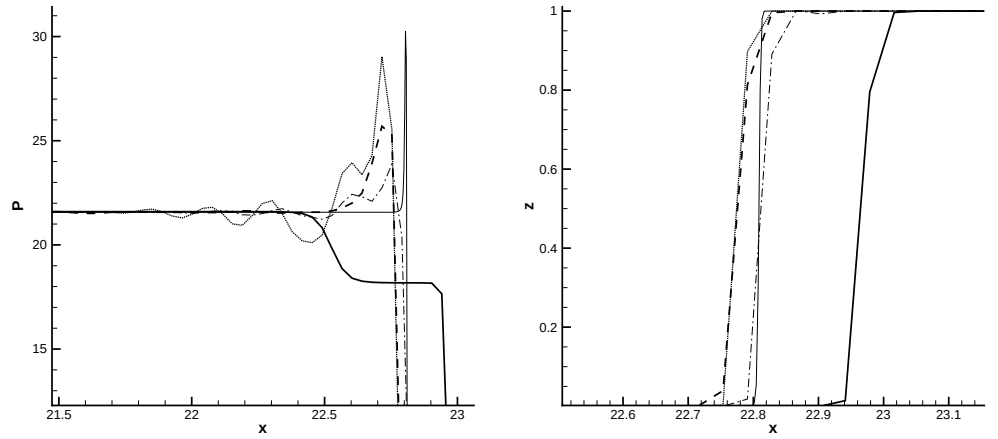

FIGURE 2. Pressure and mass fraction comparison among four high-order shock-capturing methods for the C-J detonation problem, Arrhenius case at $t = 1.8$ using 800 uniform grid points. Zoom in the vicinity of the reaction front. Thin solid line: reference solution; thick solid line: WENO5; dashed line: WENO5/SR; dashed-dot line: WENO5fi; dot line - WENO5fi+split.

in CGS units. Consider a two-dimensional channel of width 0.005 with solid walls at the upper and lower boundaries. The computational domain is $[0, 0.025] \times [0, 0.005]$. The initial conditions are

$$(\rho, u, v, p, z) = \begin{cases} (\rho_b, u_b, 0, p_b, 0), & \text{if } x \le \xi(y), \\ (\rho_u, u_u, 0, p_u, 1), & \text{if } x > \xi(y), \end{cases} \tag{4.7}$$

where

$$\xi(y) = \begin{cases} 0.004 & |y - 0.0025| \ge 0.001, \\ 0.005 - |y - 0.0025| & |y - 0.0025| < 0.001, \end{cases} \tag{4.8}$$

and $u_u = 0$, $\rho_u = 1.201 \times 10^{-3}$, $p_u = 8.321 \times 10^5$, and $u_b = 8.162 \times 10^4$. Values of p_b and ρ_b are defined by Eq. (4.1) and (4.2). In this case u_b is greater than defined by Eq. (4.4).

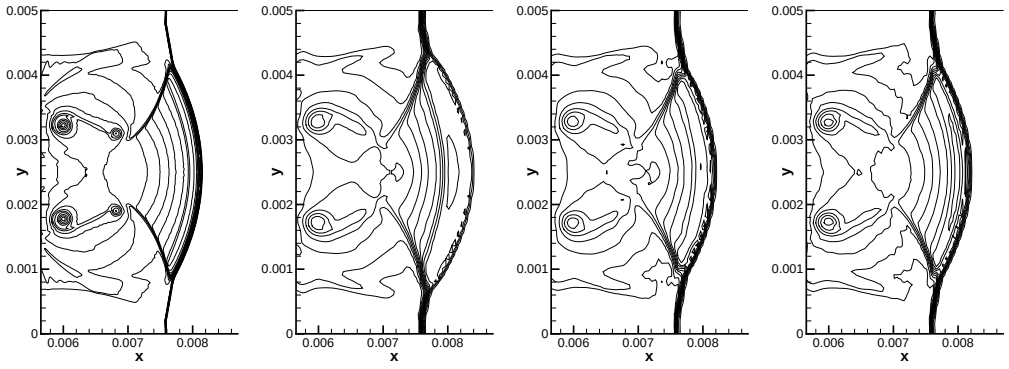

FIGURE 3. Density computed for the 2D detonation problem at $t = 0.3 \times 10^{-7}$ by different methods. From left to right: reference solution by the standard WENO5 method using 2000×400 uniform grid points; WENO5, WENO5/SR, and WENO5fi+split using 500×100 uniform grid points.

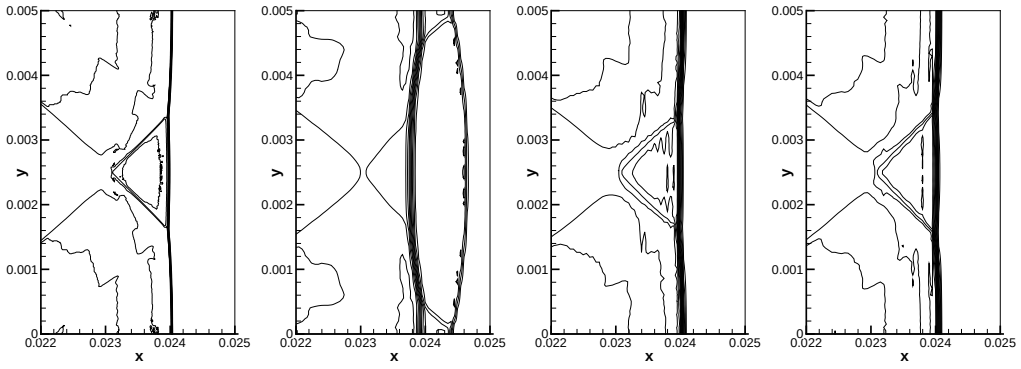

FIGURE 4. Density computed for the 2D detonation problem at $t = 1.7 \times 10^{-7}$ by different methods. From left to right: reference solution by the standard WENO5 method using 2000×400 uniform grid points; WENO5, WENO5/SR, and WENO5fi+split using 500×100 uniform grid points.

One important feature of this solution is the appearance of triple points, which travel in the transverse direction and reflect from the upper and lower walls. A discussion of the mechanisms driving this solution is given in (Kailasanath *et al.* 1985). Figures 3 and 4 show the density comparison among the standard WENO5 scheme, WENO5/SR, and WENO5fi+split, using 500×100 uniform grid points at two different times. Figures 5 and 6 show 1D cross-sections of the density compared among the standard WENO5 scheme, WENO5/SR, WENO5fi, and WENO5fi+split, using 200×40 and 500×100 uniform grid points. The reference solutions are computed by standard WENO5 with 2000×400 grid points. Again, WENO5/SR and WENO5fi+split are able to obtain the correct shock speed with similar accuracy. However, WENO5fi+split gives an oscillatory solution near $x = 0.004$ for both grids. The oscillation by WENO5fi is less pronounced than by the WENO5fi+split. WENO5 and WENO5/SR produce no oscillations at the same location.

The results for WENO5fi and WENO5fi+split are obtained by using global flow sensor.

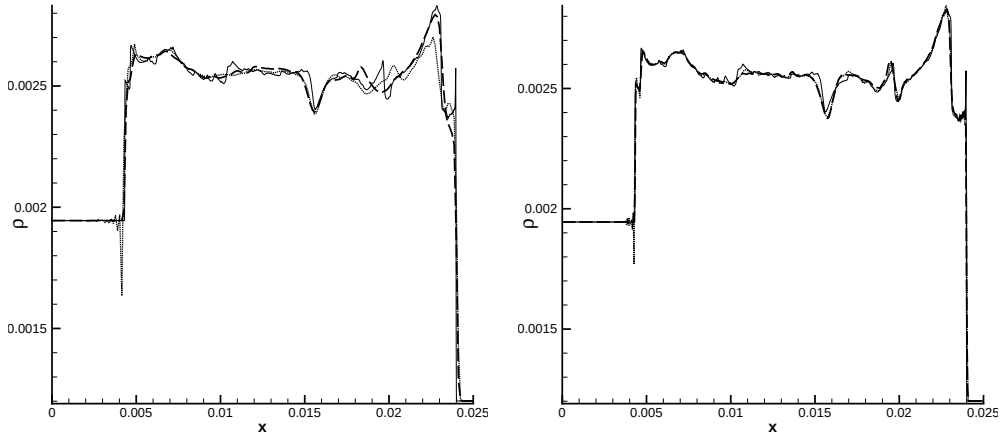

FIGURE 5. 1D cross-section of density at $t = 1.7\times10^{-7}$ by the two methods for the 2D detonation problem using 200×40 and 500×100 uniform grid points compared with the reference solution. Solid line: reference solution; dashed line: WENO5/SR; dot line - WENO5fi+split.

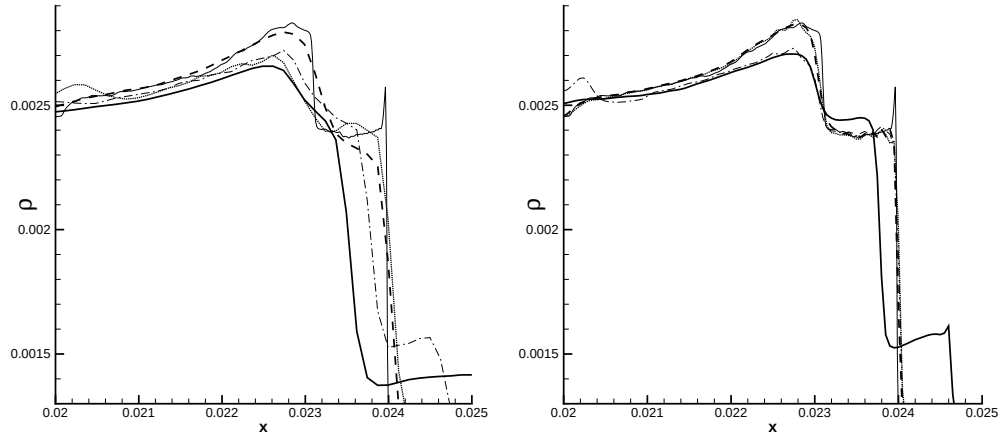

FIGURE 6. 1D cross-section of density at $t = 1.7\times10^{-7}$ by the four methods for the 2D detonation problem using 200×40 and 500×100 uniform grid points. Zoom in the vicinity of the reaction front. Thin solid line: reference solution; thick solid line: WENO5; dashed line: WENO5/SR; dashed-dot line: WENO5fi; dot line - WENO5fi+split.

By utilizing the local flow sensor (Yee & Sjögreen 2010), the oscillatory behavior near $x = 0.004$ disappears for the 200×40 grid point case and is greatly reduced for the 500×100 grid point case. The results using the local flow sensor will be reported in a forthcoming article.

5. Summary

We demonstrated that the filter version of the WENO5 in conjunction with the Ducros et al. splitting (WENO5fi+split) is able to obtain the correct propagation speed of discontinuities for two detonation problems. The accuracy is not as good as the proposed high-order finite difference schemes with subcell resolution. The next step is to examine the subcell resolution version of WENO5fi and WENO5fi+split. The combination

of these techniques (i.e. well-balanced high-order filter schemes and subcell resolution approach) might be useful for resolving the turbulent flows with fast chemical reactions.

Acknowledgments

The support of the DOE/SciDAC SAP grant DE-AI02-06ER25796 is acknowledged. The work was performed while the first author is a postdoc fellow, the fourth author was a postdoc fellow, and the fifth author was a visiting scholar at the Center for Turbulence Research, Stanford University. The financial support from the NASA Fundamental Aeronautics (Hypersonic) program for the second author is gratefully acknowledged. The work by the third author was performed under the auspices of the U.S. Department of Energy by Lawrence Livermore National Laboratory under Contract DE-AC52-07NA27344.

REFERENCES

Bao, W. & Jin, S. 2000 The random projection method for hyperbolic conservation laws with stiff reaction terms. *J. Comp. Phys.* **163**, 216–248.

Chorin, A. 1976 Random choice solution of hyperbolic systems. *J. Comput. Phys.* **22**, 517533.

Ducros, F., Laporte, F., Soulères, T., Guinot, V., Moinat, P. & Caruelle, B. 2000 High-order fluxes for conservative skew-symmetric-like schemes in structured meshes: Application to compressible flows. *J. Comp. Phys.* **161**, 114–139.

Harten, A. 1989 Eno schemes with subcell resolution. *J. Comp. Phys.* **83**, 148–184.

Helzel, C., LeVeque, R. & Warneke, G. 1999 A modified fractional step method for the accurate approximation of detonation waves. *SIAM J. Sci. Stat. Comp.* **22**, 1489–1510.

Kailasanath, K., Oran, E., Boris, J. & Young, T. 1985 Determination of detonation cell size and the role of transverse waves in two-dimensional detonations. *Combust. Flame* **61**, 199–209.

LeVeque, R. & Yee, H. C. 1990 A study of numerical methods for hyperbolic conservation laws with stiff source terms. *J. Comp. Phys.* **86**, 187–210.

Olsson, P. & Oliger, J. 1994 Energy and maximum norm estimates for nonlinear conservation laws. *Tech. Rep.* 94.01. RIACS.

Shu, C.-W. & Osher, S. 1989 Efficient implementation of essentially non-oscillatory shock-capturing schemes, ii. *J. Comp. Phys.* **83**, 32–78.

Sjögreen, B. & Yee, H. C. 2004 ultiresolution wavelet based adaptive numerical dissipation control for shock-turbulence computation. *J. Sci. Comput.* **20**, 211–255.

Sjögreen, B. & Yee, H. C. 2009*a* On skew-symmetric splitting and entropy conservation schemes for the euler equations. In *Proc. of the 8th Euro. Conf. on Numerical Mathematics & Advanced Applications (ENUMATH 2009)*. Uppsala University, Uppsala, Sweden.

Sjögreen, B. & Yee, H. C. 2009*b* Variable high order multiblock overlapping grid methods for mixed steady and unsteady multiscale viscous flows. *Commun. Comput. Phys.* **5**, 730–744.

Strang, G. 1968 On the construction and comparison of difference schemes. *SIAM J. Numer. Anal.* **5**, 506–517.

Tosatto, L. & Vigevano, L. 2008 Numerical solution of under-resolved detonations. *J. Comp. Phys.* **227**, 2317–2343.

Wang, W., Shu, C., Yee, H. C. & Sjögreen, B. 2012 High order finite difference methods with subcell resolution for advection equations with stiff source terms. *J. Comput. Phys.* **231**, 190–214.

Wang, W., Yee, H. C., Sjögreen, B., Magin, T. & Shu, C. 2011 Construction of low dissipative high-order well-balanced filter schemes for nonequilibrium flows. *J. Comput. Phys.* **230**, 4316–4335.

Yee, H. & Sjögreen, B. 2002 Designing adaptive low dissipative high order schemes for long-time integrations. In *Turbulent Flow Computation* (ed. D. D. . B. Geurts). Kluwer Academic.

Yee, H. & Sjögreen, B. 2007 Development of low dissipative high order filter schemes for multiscale Navier-Stokes/MHD systems. *J. Comput. Phys.* **225**, 910–934.

Yee, H., Vinokur, M. & Djomehri, M. 2000 Entropy splitting and numerical dissipation. *J. Comput. Phys.* **162**, 33–81.

Yee, H. C. 2002 Building blocks for reliable complex nonlinear numerical simulations. In *Turbulent Flow Computation* (ed. D. D. . B. Geurts). Kluwer Academic.

Yee, H. C., Sandham, N. & Djomehri, M. 1999*a* Low dissipative high order shock-capturing methods using characteristic-based filters. *J. Comput. Phys.* **150**, 199–238.

Yee, H. C. & Sjögreen, B. 2010 High order filter methods for wide range of compressible flow speeds. In *Proc. of ASTRONUM-2010*. San Diego, Calif, expanded version submitted to Computers & Fluids.

Yee, H. C. & Sjögreen, B. 2011 Local flow sensors in controlling numerical dissipations for a wide spectrum of flow speed and shock strength. In preparation.

Yee, H. C., Sjögreen, B. & Barone, M. 2008 High order numerical schemes for hypersonic flow simulations. In *VKI Lecture Series. Course on Hypersonic Entry and Cruise Vehicles*.

Yee, H. C., Sjögreen, B., Shu, C., Wang, W., Magin, T. & Hadjadj, A. 2011 On numerical methods for hypersonic turbulent flows. In *Proc. of ESA 7th Aerothermodynamics Symposium*. Site Oud Sint-Jan, Brugge, Belgium.

Yee, H. C. & Sweby, P. 1997 Dynamics of numerics & spurious behaviors in cfd computations. In *Keynote paper, 7th ISCFD Conf.*. Beijing, China, rIACS Technical Report 97.06, June 1997.

Yee, H. C., Torczynski, J., Morton, S., Visbal, M. & Sweby, P. 1999*b* On spurious behavior of CFD simulations. *Int. J. Num. Meth. Fluids* **30**, 675–711.